Energy Partitioning in Collisions of Slow Polyatomic Ions with Surfaces: Ethanol Molecular Ions on Surfaces Covered by Self-Assembled Monolayers (CF-SAM, CH-SAM, COOH-SAM)†

Ján Žabka, Zdenek Dolejšek, and Zdenek Herman*

V. Čermák Laboratory, J. Heyrovský Institute of Physical Chemistry, Academy of Sciences of the Czech Republic, Dolejškova 3, CZ-182 23 Prague 8, Czech Republic

Received: December 31, 2001; In Final Form: May 28, 2002

Energy transfer in ion−surface interactions between ethanol molecular ion and self-assembled monolayers formed by perfluoro-hydrocarbon (CF-SAM), hydrocarbon (CH-SAM), and hydrocarbon with terminal −COOH group (COOH-SAM) C_{11} or C_{12} chains were investigated over the incident energy range of 11−32 eV for several incident angles. Mass spectra and translational and angular distributions of product ions were used to determine distributions characterizing the partitioning of incident energy of the projectile ion into the internal excitation of the projectile, product ion translational energy, and energy absorbed by the surface. For the CF-SAM, the fraction of energy transformed into internal energy of the projectile had a maximum at about 17% of the projectile ion incident energy and did not depend on the incident angle between 40° and 80° (with respect to the surface normal); the fraction of energy in product translation was for the incident angle of 60° (measured at the product ion angular maximum) about 37%. For the CH-SAM and COOH-SAM and incident angle of 60°, the respective fractions were (peak values) 5−6% into internal excitation of the projectile, 27−30% into product translational energy, and about 64−68% absorbed by the surface, very similar as those for collisions with a hydrocarbon-covered stainless steel surface, investigated earlier.

1. Introduction

Collisions of gaseous particles with surfaces is a rapidly growing area of chemistry and physics with a wide range of applications of the results in various branches of science and technology. Collisions of slow hyperthermal ions with surfaces have been increasingly studied to provide information on dissociative processes and on chemical reactions at surfaces,[1−3] on characteristics of surfaces of various types, in particular of surfaces covered by thin films such as self-assembled monolayers (SAM),[3] on soft-landing of ions on surfaces,[4] or on modification of surfaces and thin-film production. Surface-induced dissociation (SID) of polyatomic ions has been used by organic mass spectrometrists as a tool in characterizing structural properties of organic and bioorganic ions.[2,3] Important theoretical classical trajectory simulations of polyatomic particle−surface collisions are beginning to appear.[5,6] A recent review[7] summarizes most of the present data on instrumentation and phenomena.

A number of studies have been performed on dissociative scattering of diatomic or small polyatomic (3−4 atoms) ions from single-crystal or liquid surfaces, with energy and angular analysis of the product ions. Negative ion formation in collisions of hyperthermal, state-selected NO^+ with O/Al(111)[8] and OCS^+ with Ag(111)[9] was investigated, and various mechanisms of product formation were discussed. Dissociative scattering of 50−250 eV fluorocarbon ions CF_n^+ ($n = 1-3$) from surfaces covered by a perfluoropolyether liquid film[10−12] was interpreted on the basis of elastic scattering from the surface-layer terminal group. Valuable information on collisions of very large molecular ions with surfaces came from studies of hyperthermal collisions of fullerene ions.[13−15]

Energy partitioning in collisions of gaseous particles with surfaces is an important characteristic of gas−surface interactions. In particular, the question of energy transformed in a surface collision into internal energy of a polyatomic projectile has been studied; it was estimated from the extent of fragmentation of the projectiles using various procedures[16,17] or from the fragmentation of "thermometer molecules".[18] Model calculations have been carried out to obtain information on average values of energies transferred in projectile−surface collisions.[19]

The basic energy transfer relation for a collision of a single molecular species with a surface is

$$E_{TOT} = E_{tr} + E_{int} = E'_{tr} + E'_{int} + E'_{surf} \qquad (1)$$

where E_{tr} and E_{int} are translational and internal energy of the incident projectile, respectively, and E'_{tr}, E'_{int}, and E'_{surf} are translational energy of the scattered products, energy transformed into internal excitation of the projectile, and energy absorbed by the surface, respectively (product energies primed). The respective energy fractions are characterized by their distributions, $P(E_i)$.

In our earlier papers,[20,21] we reported on studies of energy transfer in collisions of hyperthermal polyatomic ions (incident energies 10−50 eV) with a stainless steel surface[20] and carbon surfaces[21] covered by a multilayer of hydrocarbons. The effects of heating the carbon surfaces were briefly discussed, too.[21] Using the ion beam−surface scattering method and measuring mass spectra of the ion products, as well as their translational energy and angular distributions, we were able to derive distribution functions for energy partitioning in the polyatomic ion−surface collisions over the collision energy range of 10−30 eV and various projectile incident angles. The procedure was based on the following: (1) A suitable, well-characterized polyatomic ion of a small internal energy content and a well-

† Part of the special issue "R. Stephen Berry Festschrift".

* To whom correspondence should be addressed.

10.1021/jp014715f CCC: $22.00
Published on Web 08/24/2002

defined translational energy was used as a projectile impinging on a given surface. (2) Kinetic energy of the recoiling product ions was measured (at the angular maximum) to determine $P(E'_{tr})$. (3) The extent of fragmentation of the projectile ion, in combination with the break-down pattern of the ion, was used to estimate the distribution of energy converted in the interaction with the surface into the internal energy, $P(E'_{int})$. (4) The distribution of the energy absorbed in the surface, $P(E'_{surf})$, was estimated from the difference. (5) The incident angle of the projectile ion and mass spectra, translational energy distributions, and angular distribution of the scattered product ions were measured to obtain a more detailed characterization of the collisions.

Ethanol molecular ion was used as a suitable polyatomic projectile. Its advantage is that its break-down pattern, the relative abundance of the molecular and various fragment ions on the excitation energy of the molecular ion, is well-known from both theoretical[22] and experimental[23,24] studies. The relative ion abundance in the break-down pattern changes rather quickly with increasing excitation energy over the first few electronvolts, and the internal energy content of the molecular projectile ion is small. [20] In addition, the decomposition pattern of the protonated ethanol ion, formed in surface collisions as a chemical product, is relatively simple:[20] it consists of a small amount of the protonated ethanol ion, $C_2H_5OH_2^+$ ($m/z = 47$), and its decomposition products, $C_2H_5^+$ ($m/z = 29$), $C_2H_3^+$ ($m/z = 27$), and H_3O^+ ($m/z = 19$), which do not occur in the break-down pattern of the ethanol molecular ion or appear in it in negligible amounts at large excitation energies (see also Figure 3 later on). Therefore, the abundance of these ions can be subtracted from the spectrum of the unimolecular decomposition products of the molecular ion projectile.[20,21]

The described method provided data on the over-all distribution of energy in a surface collision of the molecular projectile and complemented earlier information gathered from various other approaches, both experimental and theoretical. The results for collisions with a stainless steel surface covered by hydrocarbons could be summarized as follows:[20] (1) $P(E'_{int})$ had a peak value at about 6% of E_{TOT} and its value did not change with the incident angle (50°−80° from the surface normal) and with the incident projectile energy (13−33 eV); the total width of the distribution was rather narrow extending over about 3 eV. (2) The velocity distributions of the product ions were practically the same indicating that the dissociation of the projectile ion took place after the interaction with the surface in a unimolecular way; the broadening of the velocity distributions of the fragment ions could be accounted for by a very small translational energy release (about 0.1 eV or less)[24] characterizing the unimolecular decomposition of the polyatomic ethanol molecular ion. (3) $P(E'_{tr})$, measured in the maximum of the product ion angular distribution, increased with the incident angle (peak value of 18%, 32%, and 45% at incident angles 40°, 60°, and 80°, respectively), and $P(E'_{surf})$) correspondingly decreased; the relative proportions of these fractions practically did not change over the incident energy range measured.

In this communication, we employ the described method to studies of energy transfer in collisions of polyatomic ions with chemically modified surfaces, namely, flat gold surfaces covered by self-assembled monolayers (SAM). Three types of surfaces were used: surfaces covered by C_{11} perfluoro-hydrocarbons (CF-SAM), C_{11} hydrocarbons (CH-SAM), and C_{10} hydrocarbons terminated by a COOH group (COOH-SAM). As in the earlier papers,[20,21] the ethanol molecular ion was used as a suitable model projectile. The experiments covered the range of incident projectile ion energies of 12−33 eV and incident angles of 40°−80° (from the surface normal). The distribution functions for partitioning of incident ion energy into $P(E'_{int})$, $P(E'_{tr})$, and $P(E'_{surf})$ were determined and compared with the results of the previous study (stainless steel surface with a multilayer of hydrocarbons).

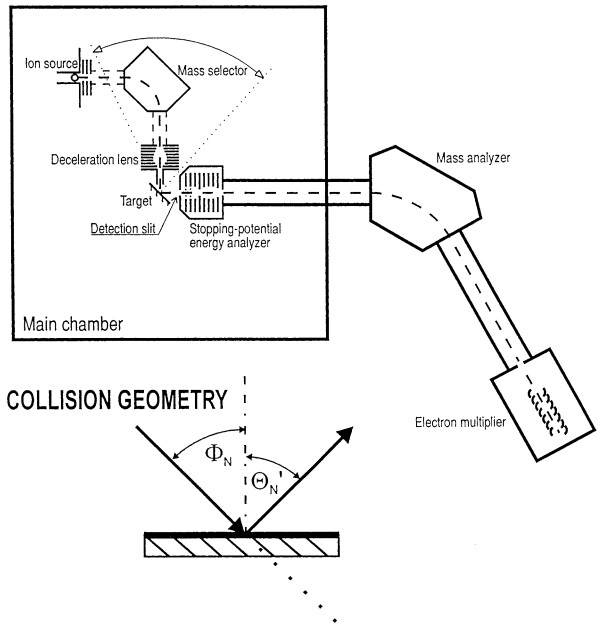

Figure 1. Schematics of the experimental apparatus. Inset defines the collision geometry.

2. Experimental Section

A modified crossed-beam scattering apparatus EVA II, built originally for studies of gas-phase ion−molecule collision dynamics, was employed in the present investigation, similarly as in our earlier ion−surface studies.[20,21,25] The modification (Figure 1) consisted of replacing the crossed beam arrangement with a solid surface target from which projectile ions were scattered and product ions registered. Projectile ions were formed by bombardment of ethanol molecules in a low-pressure ion source by 120 eV electrons. The ions were extracted, accelerated to about 140 eV, mass analyzed by a 90° permanent magnet, and decelerated to a required energy in a multielement deceleration lens. The resulting beam had an energy spread of 0.2 eV full width at half-maximum (fwhm), angular spread of 1° fwhm, and geometrical dimensions of 0.4×1.0 mm^2. The beam was directed toward the surface under a preadjusted incident angle, Φ_N. Ions scattered from the surface passed through a detection slit (0.4×1 mm^2), located 25 mm away from the target, into a stopping potential energy analyzer; they were then accelerated to 1000 eV into a detection mass spectrometer and registered with a Galileo channel multiplier. The primary beam exit slit, the target, and the detection slit were kept at the same potential during the experiments, and this equipotential region was carefully shielded by μ-metal sheets. The primary beam−target section could be rotated about the scattering center with respect to the detection slit to obtain angular distributions.

The energy of the projectile ions was measured by applying to the target a potential exceeding the nominal ion energy by about 10 eV. The target area then served as a crude ion deflector directing the projectile ions into the detection slit. Their energy could be determined with accuracy better than about 0.2 eV.

The impact angle of the projectile ions was adjusted before an experimental series by a laser beam reflection with a precision better than about 1°. Incident (Φ_N) and scattering (Θ'_N) angles were measured with respect to the surface normal (see inset in Figure 1).

The SAM samples used in this study were provided courtesy of Professor R. G. Cooks and his group (Department of Chemistry, Purdue University, West Lafayette, Indiana). The samples were[26,27] silicon wafers on which a thin layer of gold was vacuum-deposited. The surface was then treated by the respective thioalcohols, which built a self-assembled monolayer of Au−S−R with R = $(CF_2)_{10}-CF_3$ (CF-SAM), R = $(CH_2)_{11}-CH_3$ (CH-SAM), and R = $(CH_2)_{11}-COOH$ (COOH-SAM). The quality of the samples was checked by secondary-ion mass spectrometry at Purdue. The SAM surfaces were prepared as 6 × 6 mm^2 samples and kept under 100% methanol before being used. They were then mounted into the sample holder in the apparatus, which was then immediately evacuated. Experiments showed that the samples could be used for at least 24 h before showing signs of ion bombardment destruction or of a contamination (by background hydrocarbons, H-transfer reactions on the surface of CF-SAM samples). The experiments described in this paper used these freshly prepared samples.

The background pressure in the scattering apparatus was about 5×10^{-7} Torr. During the experiments, the pressure was about 2×10^{-6} Torr because of the leakage of the ethanol vapor from the source into the scattering chamber.

3. Results and Discussion

3.1. Mass Spectra. Figure 2 shows, as an example, mass spectra of products ions resulting from interaction of the projectile ethanol molecular ion of incident energy of 21−22 eV, impacting at the incident angle of 60° (with respect to the surface normal, that is, 30° with respect to the surface, measured in the angular maximum) on three surfaces covered by self-assembled-monolayers (SAM), for which we use the abbreviations (see above) CF-SAM, CH-SAM, and COOH-SAM. Similarly as in our earlier studies, one can distinguish in the spectra product ions of a different origin:[20,21] (a) product ions from unimolecular decomposition of the projectile molecular ion $C_2H_5OH^+$ (including the remaining fraction of the nondissociated molecular ion) of translational energies considerably lower than the projectile incident energy (see translational energy distributions later on); (b) product ions formed in a chemical reaction of H-atom transfer at the surface (formation of protonated ethanol $C_2H_5OH_2^+$, which almost fully decomposes to the products $C_2H_5^+$, $C_2H_3^+$, and H_3O^+ in the spectra with CH-SAM and COOH-SAM surfaces); kinetic energy of these ions is also appreciably lower than the incident projectile ion energy. Quasi-elastically scattered projectile ions (undissociated projectile ions with translational energy very close to that of the incident ions) observed earlier in collisions with $C_2H_5OH^+$ with hydrocarbon-covered stainless steel[20] or carbon[21] surfaces were not observed in measurable quantities on these SAM surfaces.

A possible interference of interactions of the projectile ion with ethanol molecules adsorbed from the background on the SAM surfaces was taken into consideration. However, the mass spectra from collisions of $C_2D_5OD^+$ (with C_2D_5OD molecules in the background) showed no indication of formation of the expected product of the surface chemical reaction between $C_2D_5OD^+$ and C_2D_5OD, the deuteronated ethanol ion $C_2D_5OD_2^+$, or its dissociation products. Therefore, we assume that the adsorption of ethanol molecules on the SAM surfaces did not play a significant role. An analogous result was observed with hydrocarbon-covered carbon surfaces.[21]

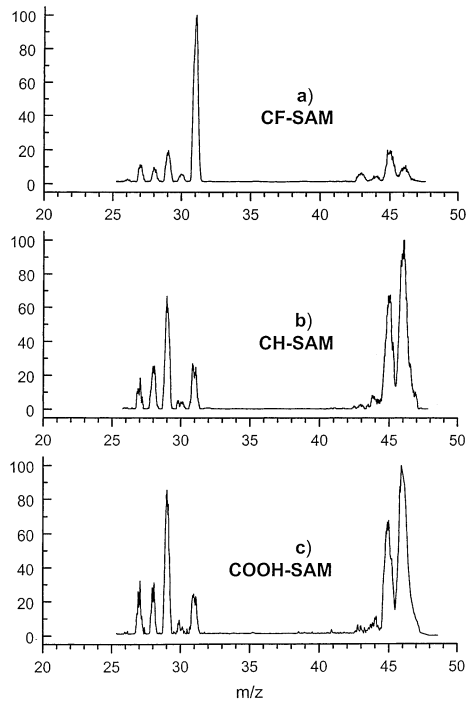

Figure 2. Mass spectra of product ions resulting from interaction of the ethanol molecular ion with surfaces covered by SAM, incident angle $\Phi_N = 60°$, $\Theta'_N = 75°$: (a) CF-SAM, $E_{tr} = 21.1$ eV; (b) CH-SAM, $E_{tr} = 21.8$ eV; (c) COOH-SAM, $E_{tr} = 22.3$ eV.

For the same incident energy and incident angle (Figure 2), the spectra obtained with CF-SAM surfaces clearly differ in the extent of fragmentation from those with CH-SAM and COOH-SAM surfaces. On the CH-SAM and COOH-SAM surfaces, the most abundant ion is the nondissociated molecular ion $C_2H_5OH^+$(m/z = 46), and considerable quantities of the fragment ion $C_2H_5O^+$ (m/z = 45) and smaller amounts of fragment ions CH_2OH^+ (m/z = 31) and C_2H_4+ (m/z = 28) are also formed. Ions of m/z = 29 and m/z = 27 are $C_2H_5^+$ and $C_2H_3^+$ coming prevailingly from a surface chemical reaction of H-atom transfer with the H-containing surface material, in agreement with our previous findings.[20,21] This conclusion was confirmed by the results of $C_2D_5OD^+$ impact, from the extent of energy transfer into internal excitation of the projectile ion, and from the characteristics of the break-down pattern of the ethanol molecular ion (see also further on).

On the other hand, the mass spectrum of the ion products from $C_2H_5OH^+$ collisions with the CF-SAM surface (Figure 2a) shows a much more pronounced fragmentation indicating a more efficient incident-to-internal energy transfer: the abundance of the molecular ion $C_2H_5OH^+$ (m/z = 46) and the fragment ion $C_2H_5O^+$ (m/z = 45) considerably decreases, and by far the most abundant product ion is CH_2OH^+ (m/z = 31). The fragment ion m/z = 29 appears to be now mostly COH^+ (the product of further decomposition of CH_2OH^+), with minor contributions of $C_2H_5^+$; the ion m/z = 27 is presumably $C_2H_3^+$ resulting from low probability of forming this product in the break-down pattern of $C_2H_5OH^+$ at high E_{int}, 6−8 eV (see the break-down pattern in Figure 3, bottom). This interpretation is consistent with analysis of mass spectra of ion products upon impact of partly or fully deuterated ethanol molecular ions.

Tables 1 and 2 summarize in a tabular form the relative abundance of product ions in the mass spectra formed in collisions of the ethanol molecular ion with the SAM surfaces.

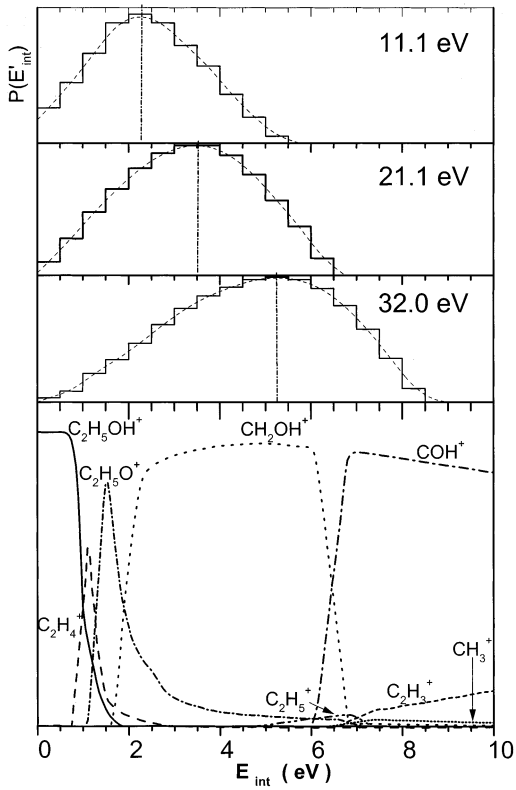

Figure 3. Distribution of energy transformed into internal excitation of the projectile ion during interaction with the surface, $P(E'_{int})$, as derived from the extent of the ethanol molecular ion fragmentation for several incident energies: CF-SAM, $\Phi_N = 60°$, $\Theta'_N = 75°$, (a) $E_{tr} = 11.1$ eV, (b) $E_{tr} = 21.1$ eV, (c) $E_{tr} = 32.0$ eV. Lower part shows the break-down pattern of the ethanol molecular ion used in the evaluation.

TABLE 1: Relative Intensities in Mass Spectra of Product Ions from Impact of $C_2H_5OH^+$ on CF-SAM and Dependence on Incident Energy for Incident Angle $\Phi_N = 60°$ from Experiment and Calculations (calcd) for $P(E'_{tr})$ Determination

	E_{tr}, 11.1 eV		E_{tr}, 21.1 eV		E_{tr}, 32.0 eV	
m/z	expt	calcd	expt	calcd	expt	calcd
46	18.5	16.2	6.6	7.3	2.3	1.8
45	19.3	21.0	13.9	14.4	8.2	6.2
44	(0.8)[a]		(2.2)[a]		(2.9)[a]	
43	(0.6)[a]		(3.5)[a]		(8.0)[a]	
31	58.6	56.5	72.6	74.9	70.0	74.2
30	(1.6)[a]		(3.1)[a]		(8.2)[a]	
29[b]	(*4.1*)[c]		(*13.9*)[c]		28.1	15.8
COH^+[b]					11.2	15.3
$C_2H_5^+$[b]					(*16.9*)[c]	0.5
28	3.6	6.3	6.9	3.4	8.3	1.0
27	(*0.4*)[c]		(*9.4*)[c]		(*7.1*)[c]	
26			(1.0)[a]		(7.3)[a]	
19	(*0.4*)[c]		(*0.6*)[c]		(*1.9*)[c]	
15			(0.5)[a]		(0.3)[a]	0.3

[a] Values in parentheses are relative intensities of product ions not considered in fit calculations of $P(E'_{int})$. [b] Total intensity of $m/z = 29$ and relative contributions of COH^+ and $C_2H_5^+$ to it (as estimated from deuterated ethanol ion collisions). [c] Value in italics in parentheses are product ions from surface chemical reaction not considered in calculations of $P(E'_{int})$.

Both experimental and calculated abundance used in the $P(E'_{int})$ determination are given in the tables. Product ions of very low abundance (numbers in parentheses) and ions formed in surface chemical reactions (italics in parentheses) were not used in the fitting procedure.

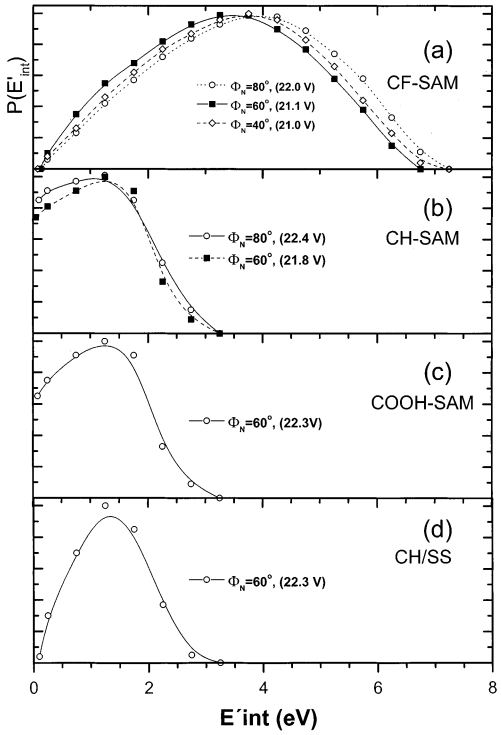

Figure 4. Distribution of energy transformed in the surface collision into the internal excitation of the projectile ion, $P(E'_{int})$, for various incident angles Φ_N on surfaces covered by (a) CF-SAM, (b) CH-SAM, (c) COOH-SAM, and (d) for hydrocarbon-covered stainless steel (CH/SS). [20] Incident angle Φ_N and incident energies (in parentheses) are given in the figure. Mass spectra were measured at the product ion angular maxima.

The fragmentation data were used to estimate the distribution of energy transformed into internal energy of the projectile ion during its interaction with the surface, $P(E'_{int})$. The break-down pattern of the ethanol molecular ion was used to fit the relative intensities of the ion species in the mass spectra by a trial-and-error distribution function, $P(E'_{int})$, using the expression

$$I_i = \int P(E'_{int}) A_i(E'_{int})\, dE'_{int} \qquad (2)$$

where $A_i(E'_{int})$ is the abundance of the ion species i in the break-down pattern at E_{int}. The break-down pattern of the ethanol molecular ion[12−14] used in the evaluation is given in the bottom part of Figure 3.

Figures 3 and 4 show the $P(E'_{int})$ that gave the best fit with the experimental mass spectra. Figure 3 (see also Table 1) summarizes the data for the CF-SAM surface in dependence on the collision energy between 11 and 32 eV and for the incident angle $\Phi_N = 60°$. Figure 4 brings the data on $P(E'_{int})$ obtained at collision energies 21−22 eV for the CF-SAM surface in dependence on the incident angle (Figure 4a) and data for CH-SAM (Figure 4b) and COOH-SAM (Figure 4c) for the indicated incident angles (see also Table 2). For comparison, the $P(E'_{int})$ curve obtained earlier from data on the hydrocarbon-covered stainless steel surface (CH/SS) for a comparable collision energy and incident angle is given, too (Figure 4d).

The data in Figure 3 show that for the CF-SAM surface the fraction of incident energy transformed into the internal energy of the projectile, $P(E'_{int})$, increases linearly with collision energy (peak values 2.3, 3.5, and 5.3 eV for collision energies of 11.1, 21.1., and 32.0 eV, respectively, that is, 21−17% of the incident energy). The total width of the distribution $P(E'_{int})$ increases from about 5.5 to about 8.5 eV over this

TABLE 2: Relative Intensities in Mass Spectra of Product Ions from Impact of $C_2H_5OH^+$ on Various SAM Samples and Various Angles at Incident Energy = 21.2−22.4 eV from Experiments and Calculations (calcd) for $P(E'_{tr})$ Determination

	CF-SAM surface				CH-SAM surface				COOH-SAM surface	
	E_{tr} = 21.2 eV, Φ_N = 40°		E_{tr} = 22.0 eV, Φ_N = 80°		E_{tr} = 21.8 eV, Φ_N = 60°		E_{tr} = 22.4 eV, Φ_N = 80°		E_{tr} = 22.3 eV, Φ_N = 60°	
m/z	expt	calcd	expt	calcd	expt	calcd	expt	calcd	expt	calcd
46	5.0	6.5	5.2	5.6	46.8	46.2	47.8	46.7	46.0	47.5
45	19.3	13.8	9.8	12.5	30.5	25.7	23.2	29.6	32.4	26.3
44	(2.7)[a]		(1.2)[a]		(4.1)[a]		(2.4)[a]		(2.9)[a]	
43	(5.6)[a]		(1.4)[a]		(1.0)[a]		(0.9)[a]		(1.3)[a]	
31	72.6	76.8	80.8	77.8	11.1	13.2	14.8	15.0	10.4	9.6
30	(2.9)[a]		(3.0)[a]		(2.6)[a]		(2.3)[a]		(3.3)[a]	
29	*(19)*[b]		*(7.5)*[b]		*(27.3)*[b]		*(22.2)*[b]		*(39)*[b]	
28	8.1	3.1	4.0	4.0	11.4	14.9	8.6	13.7	11.2	(16.6)[a]
27	*(18)*[b]		*(3.7)*[b]		*(4.2)*[b]		*(3.1)*[b]		*(10.5)*[b]	
26										
19	*(22)*[b]		*(0.6)*[b]		*(7.6)*[b]		*(6.4)*[b]		*(8.9)*[b]	

[a] Values in parentheses are relative intensities of product ions not considered in calculations of $P(E'_{int})$. [b] Values in italics in parentheses are product ions from surface chemical reactions not considered in calculations of $P(E'_{int})$.

collision energy range. Figure 4 provides a comparison for the fraction of energy transformed into internal energy for collisions with different surfaces. For the CH-SAM and COOH-SAM surfaces, the $P(E'_{int})$ curves peak at about the same value of 1.3 eV (about 6% of the incident energy), and the data are rather similar to the data for the hydrocarbon-covered stainless steel surface. [10] However, the $P(E'_{int})$ curves for the CF-SAM surface are strikingly different, much broader and with a peak at considerably higher energy of 3.3−3.8 eV, indicating about 3-times more-efficient incident-to-internal energy conversion with this surface than with the other surfaces. The data for CF-SAM and different incident angle (Figure 4a) confirm for this surface the earlier findings[10] that the incident-to-internal energy transfer is practically independent of the incident angle of the projectile ions.

The data on the peak value of the incident-to-internal energy transfer for the CF-SAM surface (about 17% of the incident energy) are in good agreement with the earlier reported average energy transfer from other measurements;[18] the peak values for the other surfaces (6% of the incident energy for CH-SAM, COOH-SAM, and hydrocarbon-covered stainless steel) are lower than those from reports from other mass spectrometric measurements (average value of about 12% of the incident energy,[19] but they are in reasonable agreement with recent data on fullerene ion−hydrocarbon-covered stainless steel collisions (6.8%)[15] and recent classical trajectory simulations of collisions of large polyatomic ions with CH-SAM type surfaces (7−8%).[5]

3.2. Translational Energy Distributions of Product Ions. Translational energy distributions were measured for all major product ions resulting from the interaction of the projectile ion $C_2H_5OH^+$ with the three SAM surfaces at the investigated incident energies and incident angles. Figure 5a shows, as an example, the translational energy distributions of product ions m/z = 46 (nondissociated $C_2H_5OH^+$), m/z = 45 ($C_2H_5O^+$), and m/z = 31 (CH_2OH^+) formed upon impact of the projectile ion $C_2H_5OH^+$ on the CF-SAM surface at the incident energy of 22.6 eV and incident angle Φ_N = 60°, measured close to the maximum of the angular distributions, Θ'_N = 75°. In all cases, the translational energy is much lower than the incident energy, indicating a strongly inelastic process. The peak of the energy distribution shifts to lower energies with decreasing mass of the product ion. In Figure 5b, the same distributions are plotted as the function of product ion *velocity* rather than translational energy. The maxima of the distributions then occur at the same velocity of about 6.2 km/s, and the distributions have a very similar shape. This suggests, in agreement with our previous findings[20,21,25] and with the results of others,[28,29] that the fragmentation of the projectile molecular ion, excited in an inelastic collision with the surface, occurs in a unimolecular way *after* the interaction with the surface. The product ions should then have the velocity distribution of the undissociated molecular ion (scattered inelastically from the surface), possibly broadened (m/z = 31) by the translational energy release in the dissociation process; this energy release is known, however, to be rather small for the ethanol molecular ion and the dissociations in question (about 0.1 eV or less).[24]

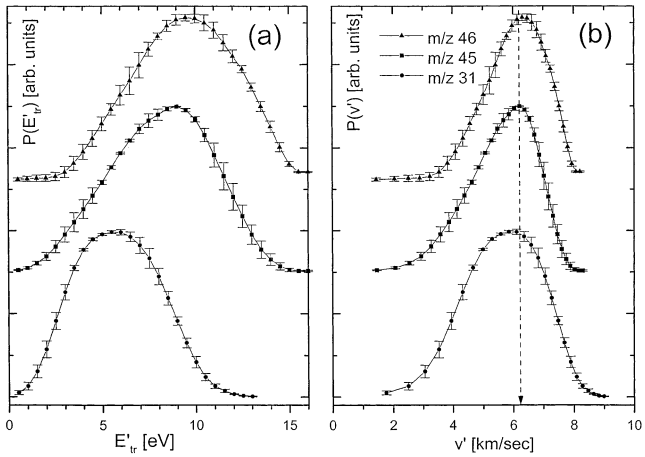

Figure 5. Translational energy distributions (a) and velocity distributions (b) of major product ions m/z = 46 ($C_2H_5OH^+$), m/z = 45 ($C_2H_5O^+$), and m/z = 31 (CH_2OH^+) formed in the interaction of the ethanol molecular ion with the surface covered by CF-SAM. Incident energy E_{tr} = 22.6 eV, incident angle Φ_N = 60°, and Θ'_N = 75° (angular maximum).

Figure 6 shows analogous velocity distributions of the product ions formed in collisions of the projectile ion $C_2H_5OH^+$ under analogous incident energy and incident angle with other SAM surfaces, namely, for the CH-SAM surface (Figure 6a) and for the COOH-SAM surface (Figure 6b). The results lead to the same conclusion as above, except that the peak velocity of the distributions is somewhat smaller than in the case of the CF-SAM surface (5.2 km/sec, the incident ion velocity is 9.65 km/sec). These findings provide justification for using the translational energy distribution of the undissociated molecular ion, scattered inelastically from the surface, as representing the translational energy distribution term, $P(E'_{tr})$, in the determination of energy partitioning.

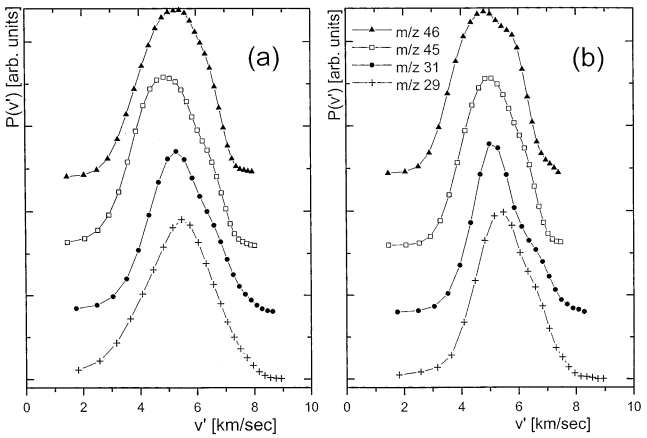

Figure 6. Velocity distributions of major product ions formed in the interaction of the ethanol molecular ion with the surface covered by (a) CH-SAM (E_{tr} = 21.8 eV, $\Phi_N = 60°$, $\Theta'_N = 75°$) and (b) COOH-SAM (E_{tr} = 22.3 eV, $\Phi_N = 60°$, $\Theta'_N = 70°$).

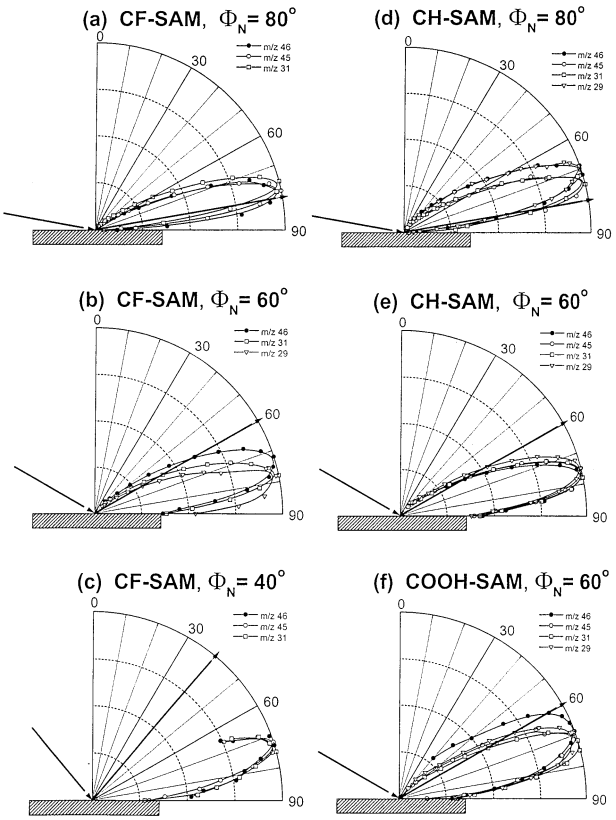

Figure 7. Angular distributions of major product ions formed in the interaction of the ethanol molecular ion with surfaces covered by SAM as a function of the incident angle for incident energy of 21.1−22.4 eV: (a) CF-SAM, $\Phi_N = 80°$; (b) CF-SAM, $\Phi_N = 60°$; (c) CF-SAM, $\Phi_N = 40°$; (d) CH-SAM, $\Phi_N = 80°$; (e) CH-SAM, $\Phi_N = 60°$; COOH-SAM, $\Phi_N = 60°$. Incident angle and specular reflection angle are denoted by arrows.

3.3. Angular Distributions of Product Ions. Polar plots of angular distributions of product ions from interaction of the molecular projectile ions $C_2H_5OH^+$ of incident energy of about 22 eV with surfaces covered by various self-assembled monolayers are given in Figure 7. Figure 7a−c shows the results for impact on CF-SAM surfaces under three different incident angles of 80°, 60°, and 40°. Figure 7d,e shows the results for impact on the CH-SAM surface under incident angles of 80° and 60°, and finally, Figure 7f shows the results for impact on a COOH-SAM surface under $\Phi_N = 60°$. Similarly as in our previous study with the hydrocarbon-covered stainless steel surface, [20] the maximum of the inelastically scattered ion intensity appears to occur, depending on the incident angle, at smaller or larger angle than the specular angle, or close to it. The difference is that the recoil angle is in general larger (i.e., closer to the surface) for the SAM surfaces than it was for the hydrocarbon-covered stainless steel. The difference seems to be largest for the CF-SAM surface. For example, the angular distributions with the hydrocarbon-covered stainless steel surface peaked at 68°, 62°, and 58° for the incident angles of 80°, 60°, and 40°, respectively,[20] while for the CF-SAM surfaces the angular maxima are located at 78°, 72−75°, and 72°, for the same incident angles, respectively. This suggests that the SAM surfaces tend to behave like somewhat "softer" surfaces than the hydrocarbon-covered stainless steel surface.

To correlate the positions of the angular maxima and the maxima of the translational energy distributions of the scattered product ions, we introduced in our earlier paper[20] simple relations between the velocity components of the impinging projectile ions and the scattered projectile ions. The velocity of the projectile ion (impinging under a certain incident angle Φ_N), v, and the peak velocity of the inelastically scattered product ions (at the angular maximum Θ'_N), v', were decomposed into velocity component perpendicular ($v_\perp$,$v'_\perp$) and parallel ($v_{||}$,$v'_{||}$) to the surface (primed quantities refer to products),

$$v_\perp = v \cos \Phi_N \qquad v'_\perp = v' \cos \Theta'_N \qquad (3a,b)$$

$$v_{||} = v \sin \Phi_N \qquad v'_{||} = v' \sin \Theta'_N \qquad (3c,d)$$

For collisions of the ethanol molecular ion with a stainless steel surface covered by a multilayer of hydrocarbons, it was found[20] that (i) the ratio of the most probable parallel velocities of the scattered and incident ion, $v'_{||}/v_{||}$, was independent of the incident angle and equal to 0.7 and (ii) the value of the product ion perpendicular velocity, $v'_\perp$, was a constant not dependent on the projectile ion incident angle but dependent on the collision energy; for the incident energy of 22.3 eV, it was 2.6 km/s, and for the incident energy of 32.7 eV, it was 3.1 km/s. [20]

Figure 8 shows the plot of the parallel and perpendicular velocity component relations in dependence on the projectile incident angle for the various SAM surfaces at the projectile energy of 21.6−22.3 eV as derived from the data of this paper. Dashed lines indicate the earlier published data[20] for the ethanol molecular ion projectiles impinging on a hydrocarbon-covered stainless steel surface (experimental points given in ref 10 were omitted). It can be seen from Figure 8 that the parallel velocity relation is practically the same for the three SAM surfaces as for the hydrocarbon-covered stainless steel, leading to $v'_{||}/v_{||} = 0.7$. The value of $v'_\perp$ is, however, considerably smaller for the CF-SAM, CH-SAM, and COOH-SAM than for the hydrocarbon-covered stainless steel, roughly independent of the incident angle and approximately equal to 1.5 km/s.

In a simple model, the energy loss of the scattered particles may be regarded as resulting from a binary collision of the projectile with an effective mass of the surface.[10,30] Applying kinematic formulas of energy and momentum conservation leads to the expression for the energy of the projectile ion[1,10]

$$E'_{tr} = E_{tr}[\cos \theta \pm (A^2 - \sin^2 \theta)^{1/2}]^2/(1 + A)^2 \qquad (4)$$

where E_{tr} and E'_{tr} is translational energy of the incident and scattered particle, respectively, θ is the total scattering angle (defined as the deviation from the original beam direction and

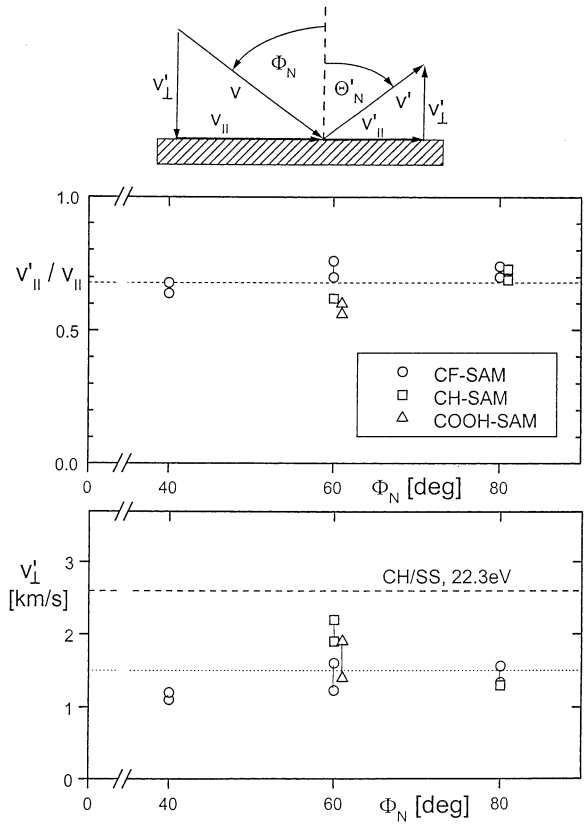

Figure 8. Dependence of the velocity components of the incident ethanol molecular ion (incident energy 21.1−22.4 eV) and inelastically scattered product (undissociated molecular ion) on the incident angle Φ_N. Θ'_N refers to the angular maxima. The dashed lines are from ref 8 (without experimental points) and refer to collisions of the ethanol molecular ion with a hydrocarbon-covered stainless steel (CH/SS) surface (22.3 eV). Inset shows the relations between the velocity components.

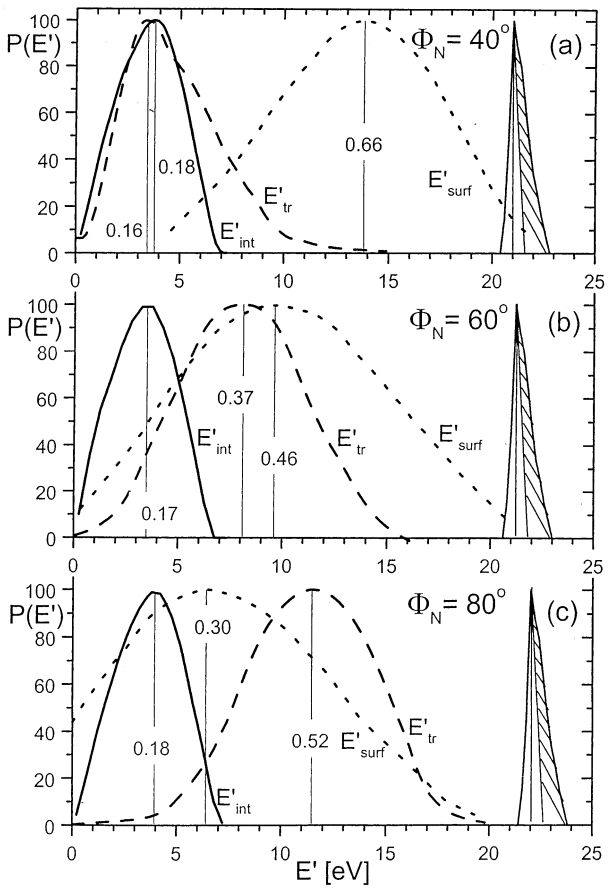

Figure 9. Distribution functions for energy partitioning into E'_{int}, E'_{tr}, and E'_{surf} from collisions of the ethanol molecular ion with the CF-SAM surface for incident projectile ion angle Φ_N of (a) 40°, (b) 60°, and (c) 80°. Projectile incident energy was 21−22 eV, measured at the angular maxima. Hatched area represents the estimated internal energy distribution of the projectile ion.

refers to the maximum of the angular distribution), and $A = M_T/M_P$ (M_P is the mass of the projectile, $M_P = 46$, and M_T is the "effective" mass of the target). For the CF-SAM surface and incident angles Φ_N of 40°, 60°, and 80°, one gets from the data $M_T = 47$, 35, and 17, respectively; for the CH-SAM surface and $\Phi_N = 60°$, one obtains $M_T = 31$. The values of M_T seem to be rather far from the masses of the terminal groups of the surfaces (69 for CF_3- of the CF-SAM, 15 for CH_3- of the CH-SAM) and vary largely with the incident angle. This suggests that a simple two-body scattering model does not describe adequately the collision of the ethanol projectile on the SAM surfaces in the collision energy range studied. This may not be surprising because results of recent trajectory calculations on collisions of polyatomic projectile ions with SAM surfaces indicate that the energy transfer occurs as a rather complex multimode excitation process in a short-duration collision and dissociation of the projectile takes place after intramolecular vibrational energy redistribution in accord with the Rice−Ramsperger−Kassel−Marcus (RRKM) theory.[5,6,31]

3.4. Incident Energy Partitioning. From the experimental data reported here, one can derive the distributions for energy partitioning in collisions of ethanol molecular ions with CF-SAM, CH-SAM, and COOH-SAM surfaces. The same approach was used here as in our earlier papers,[20,21] that is, the respective energy distributions were introduced into the energy transfer eq 1. For the incident ion translational energy distribution, $P(E_{tr})$, the projectile ethanol molecular ion energy distribution was used as measured. The internal energy distribution of the projectile ion, $P(E_{int})$, was estimated as a product of the range of stability of the undissociated molecular ion, derived from its break-down pattern (see Figure 3), and the probability of populating internal energy states of the molecular ion in this range, obtained from ethanol photoelectron spectra[32] (assuming that the population of the internal states by 120 eV electron impact was approximately the same as in photoionization). The term $P(E'_{tr})$ was taken as the measured translational energy distributions of the inelastically scattered undissociated molecular product ion at its angular maximum (Figures 5 and 6). The $P(E'_{tr})$ are averages of a series of product ion translational energy measurements. The distribution of energy transformed into internal energy of the projectile ion, $P(E'_{int})$, was obtained from the extent of the surface-excited projectile ion fragmentation (see section 3.1 and Figures 3 and 4). The distribution $P(E'_{surf})$ was taken as a difference of all these terms.

Figure 9 summarizes the data for energy partitioning in collisions of the ethanol molecular ion projectile (incident energy 21−22 eV) with CF-SAM surfaces for three different projectile ions incident angles Φ_N. The data refer to energy partitioning at the product ion angular maxima. The results show that the fraction of energy transformed into the internal energy of the surface-excited projectile ion, $P(E'_{int})$, was practically independent of the incident angle with a peak value of 17−18% of the incident energy and a full width at half-maximum (fwhm) of about 4.1 eV(19% of the incident energy). The fraction of energy in product ion translation increased with the incident angle from the peak value of 16% at $\Phi_N = 40°$ to 52% of the incident

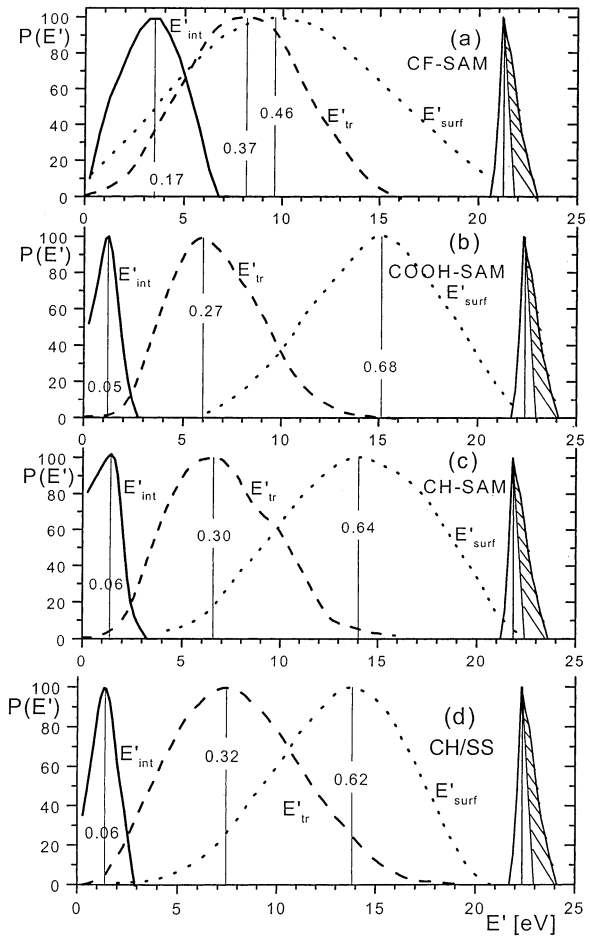

Figure 10. Comparison of distribution functions for energy partitioning into E'_{int}, E'_{tr}, and E'_{surf} from collisions of the ethanol molecular ion with (a) CF-SAM, (b) CH-SAM, (c) COOH-SAM, and (d) hydrocarbon-covered stainless steel surface (CH/SS). Incident energy = 21.2−22.4 eV, incident angle $\Phi_N = 60°$, measured at the angular maxima (Θ'_N = 75°−70°).

energy at $\Phi_N = 80°$, with fwhm of 5−8 eV (22−36% of the incident energy). The distribution of the fraction of energy absorbed by the surface, $P(E'_{surf})$, correspondingly decreased from 66% to 30% of its peak value. It is interesting to note a nonnegligible probability of zero energy transfer to the surface in collisions close to glancing collisions ($\Phi_N = 80°$, that is, 10° with respect to the surface).

Finally, Figure 10 brings a comparison of energy partitioning in collisions of the ethanol molecular ion of the same incident energy (21−22 eV) and the same incident angle ($\Phi_N = 60°$) with surfaces covered by various self-assembled monolayers (CF-SAM, CH-SAM, and COOH-SAM) and, for comparison, with the hydrocarbon-covered stainless steel surface. [20] Again, the data refer to energy partitioning at the product ion angular maxima. It can be seen that the CH-SAM and the COOH-SAM surfaces give very similar results for energy partitioning as the hydrocarbon-covered stainless steel. In particular, a comparison between the CH-SAM and the hydrocarbon-covered stainless steel indicates that the self-assembled C_{12} hydrocarbon chain monolayer (CH-SAM) has very similar properties (as far as energy partitioning is concerned) as the random adsorbed multilayer of hydrocarbons on a stainless steel surface. The CF-SAM system is different in that the fraction of energy transformed into the surface-excited projectile internal energy is about 3-times higher than that on the other surfaces in Figure 10 (peak value of 17% vs 5−6% of the incident energy, respectively). Also, the fraction of energy going into product ion translation appears to be larger for the CF-SAM surface, and the fraction of energy absorbed by the surface correspondingly smaller (peak value of 40% for CF-SAM and 27−32% for CH-SAM and COOH-SAM of the incident energy).

4. Conclusions

The ion−surface scattering method was used to obtain data on energy partitioning in collisions of the ethanol molecular ion (collision energy range 11−32 eV, incident angle 40°, 60°, and 80° with respect to the surface normal) with surfaces covered by self-assembled monolayers of different types (CF-SAM, CH-SAM, COOH-SAM). Mass spectra of the product ions, translational energy distributions, and angular distributions of the product ions were determined.

Distribution of energy transferred into internal energy of the projectile, $P(E'_{int})$, was determined from the extent of fragmentation of the surface-excited projectile ion with the use of the break-down pattern of the projectile molecular ion. Distribution of translational energy of the product ions, $P(E'_{tr})$, was measured directly at the angular maximum. Distribution of energy absorbed by the surface, $P(E'_{surf})$, was obtained as a difference of the sum of these two terms and the incident energy of the projectile (with the estimated internal energy of the projectile included).

The value of $P(E'_{int})$ differs considerably for the CF-SAM, and it is about 3-times larger than that for the CH-SAM and COOH-SAM surfaces, for which it has a peak value of 5−6%, similarly as for the hydrocarbon-covered stainless steel surface. The value of $P(E'_{int})$ does not seem to depend on the incident angle of the projectile ion.

The over-all energy partitioning at the product ion angular maximum for the same incident energy (21−22 eV) and the same incident angle (60° from the surface normal) seems to be very similar for the CH-SAM and COOH-SAM surfaces and the hydrocarbon-covered stainless steel surface with peak values of $P(E'_{int}) = 5-6\%$, of $P(E'_{tr}) = 27-32\%$, and $P(E'_{surf}) = 62-68\%$ of the incident energy. The CF-SAM surface shows, for the same incident ion parameters, a considerably larger fraction of energy in internal energy of the projectile (peak value of $P(E'_{int})$ is 17%) and translational energy of the products (peak value of $P(E'_{tr})$ is 37%) and a correspondingly smaller fraction of energy absorbed by the surface (peak value about 40% of the incident energy).

Acknowledgment. The paper is dedicated to R. Stephen Berry as an expression of our respect to his personality and to his manifold contributions to science. The authors wish to thank R. Graham Cooks (Purdue University, West Laffayette, IN) and co-workers for the invaluable gift of characterized samples of the CF-SAM, CH-SAM, and COOH-SAM surfaces used in the experiments. The help of Jana Roithová in evaluating the $P(E'_{int})$ distributions was much appreciated. Partial support of this research by the Grant Nos. 203/97/0351 and 203/00/0632 of the Grant Agency of the Czech Republic is gratefully acknowledged.

References and Notes

(1) Rabalais, J. W., Ed. *Low Energy Ion-Surface Interactions*; John Wiley: New York, 1994.

(2) Cooks, R. G.; Ast, T.; Mabud, M. D. A. *Int. J. Mass Spectrom. Ion Processes* **1990**, *100*, 209.

(3) Hanley, L., Ed. Polyatomic-Surface Interactions. *Int. J. Mass Spectrom.* **1998**, *174*.

(4) Miller, S. A.; Luo, H.; Pachuta, S. J.; Cooks, R. G. *Science* **1997**, *273*, 1447.
(5) Meroueh, O.; Hase, W. L. *Phys. Chem. Chem. Phys.* **2001**, *3*, 2306.
(6) Meroueh, O.; Hase, W. L. *J. Am. Chem. Soc*., in press.
(7) Grill, V.; Shen, J.; Evans, C.; Cooks, R. G. *Rev. Sci. Instrum*. **2001**, *72*, 3149.
(8) Morris, J. R.; Kim, G.; Barstis, T. L. O.; Mitra, R.; Jacobs, D. C. *J. Chem. Phys.* **1997**, *107*, 6448.
(9) Maazous, M.; Barstis, T. L. O.; Maazous, P. L.; Jacobs, D. C. *Phys. Rev. Lett.* **2000**, *84*, 1331.
(10) Koppers, W. R.; Beijersbergen, J. H. M.; Weeding, T. L.; Kistemaker, P. G.; Kleyn, A. W. *J. Chem. Phys.* **1997**, *107*, 10736.
(11) Koppers, W. R.; Gleeson, M. A.; Lourenco, J.; Weeding, T. L.; Los, J.; Kleyn, A. W. *J. Chem. Phys.* **1999**, *110*, 2588.
(12) Los, J.; Gleeson, M. A.; Koppers, W. R.; Weeding, T. L.; Kleyn, A. W. *J. Chem. Phys.* **1999**, *111*, 11080.
(13) Beck, R. D.; Rockenberger, J.; Weiss, P.; Kappes, M. M. *J. Chem. Phys.* **1996**, *104*, 3638.
(14) Bekkerman, A.; Tsipinyuk, B.; Verkhoturov, S.; Kolodney, E. *J. Chem. Phys.* **1998**, *109*, 8652.
(15) Biasioli, F.; Fiegele, T.; Mair, C.; Herman, Z.; Echt, O.; Aumayr, F.; Winter, H. P.; Märk, T. D. *J. Chem. Phys.* **2000**, *113*, 5053.
(16) Kenttämaa, H. I.; Cooks, R. G. *Int. J. Mass Spectrom. Ion Processes* **1985**, *64*, 79.
(17) Vékey, K.; Somogyi, A.; Wysocki, V. H. *J. Mass Spectrom.* **1995**, *30*, 212.
(18) Wysocki, V. H.; Kenttämaa, H. I.; Cooks, R. G. *Int. J. Mass Spectrom. Ion Processes* **1987**, *75*, 181.
(19) Wainhaus, S. B.; Gislason, E. A.; Hanley, L. *J. Am. Chem. Soc.* **1997**, *119*, 4001.
(20) Kubišta, J.; Dolejšek, Z.; Herman, Z. *Eur. Mass Spectrom.* **1998**, *4*, 311.
(21) Žabka, J.; Dolejšek, Z.; Roithová, J.; Grill, V.; Märk, T. D.; Herman, Z. *Int. J. Mass Spectrom.* **2002**, *213*, 145.
(22) Friedman, L.; Long, F. A.; Wolfsberg, M. *J. Chem. Phys.* **1957**, *27*, 613.
(23) von Koch, H.; Lindholm, E. *Ark. Fys.* **1961**, *19*, 123.
(24) Niwa, Y.; Nishimura, T.; Tsuchiya, T. *Int. J. Mass Spectrom. Ion Phys.* **1982**, *42*, 91.
(25) Wörgötter, R.; Kubišta, J.; Žabka, J.; Dolejšek, Z.; Märk, T. D.; Herman, Z. *Int. J. Mass Spectrom. Ion Processes* **1998**, *174*, 53.
(26) Luo, H.; Miller, S. A.; Cooks, R. G.; Pachuta, S. J. *Int. J. Mass Spectrom. Ion Processes* **1998**, *174*, 193.
(27) Wade, N.; Evans, C.; Pepi, F.; Cooks, R. G. *J. Phys. Chem. B* **2000**, *104*, 11230.
(28) Morris, M.; Riederer, D. E.; Winger, B. E.; Cooks, R. G.; Ast, T.; Chidsey, C. E. D. *Int. J. Mass Spectrom. Ion Processes* **1992**, *122*, 181.
(29) Burroughs, J. A.; Wainhaus, S. A.; Hanley, L. *J. Phys. Chem.* **1994**, *98*, 10913.
(30) De Clerq, H. L.; Sen, A. D.; Shukla, A. K.; Futrell, J. H. *Int. J. Mass Spectrom.* **2001**, *212*, 491.
(31) Hase, W. L. Private communication.
(32) Kimura, K.; Katsumata, S.; Achiba, Y.; Yamazaki, T.; Iwata, S. *Handbook of HeI Photoelectron Spectra of Fundamental Organic Molecules*; Japan Scientific Society Press: Tokyo, 1981.